 doi:10.20944/preprints202107.0517.v1

Article

Numerical study on the fluid flow and heat transfer characteristics of Al_2O_3-water nanofluids in microchannels of different aspect ratio

Huajie Wu [1],Shanwen Zhang [2]

[1] Yangzhou polytechnic institute, Jiangsu 225127, China
[2] College of Mechanical Engineering, Yangzhou University, Jiangsu 225127, China

Abstract: The study of the influence of the nanoparticle volume fraction and aspect ratio of microchannels on the fluid flow and heat transfer characteristics of nanofluids in microchannels is important in the optimal design of heat dissipation systems with high heat flux. In this work, the computational fluid dynamics method was adopted to simulate the flow and heat transfer characteristics of two types of water–Al_2O_3 nanofluids with two different volume fractions and five types of microchannel heat sinks with different aspect ratios. Results showed that increasing the nanoparticle volume fraction reduced the average temperature of the liquid–solid heat transfer interface and thereby improved the heat transfer capacity of the nanofluids. Meanwhile, the increase of the nanoparticle volume fraction led to a considerable increase in the pumping power of the system. Increasing the aspect ratio of the microchannel effectively improved the heat transfer capacity of the heat sink. Moreover, increasing the aspect ratio effectively reduced the average temperature of the heating surface of the heat sink without significantly increasing the flow resistance loss. When the aspect ratio exceeded 30, the heat transfer coefficient did not increase with the increase of the aspect ratio. The results of this work may offer guiding significance for the optimal design of high heat flux microchannel heat sinks.

Keywords: Microchannel; Nanofluid; Heat transfer enhancement; Numerical simulation

1. Introduction

With the continuous miniaturization and integration of electronic devices, the heat flux density continues to increase, and conventional cooling methods are no longer effective. Therefore, the heat dissipation problem of high heat flux density has been a research hotspot in the field of heat transfer, [1-2]. In 1981, Tuckerman and Pease[3] proposed a silicon microchannel heat sink, which uses deionized water as a liquid cooling medium and whose heat dissipation capacity can be as high as 790 W/cm^2. In 1995, Choi and Eastman[4] proposed the concept of nanofluids; a certain proportion of solid particles with a diameter of less than 100 nm was added into a base fluid with low thermal conductivity, and the suspension with high thermal conductivity was found to be relatively stable. This special liquid can significantly improve the convective heat transfer capacity of cooling media. The addition of nanoparticles, to high-Prandtl number liquids significantly increases the heat transfer performance of micro heat-sinks. and treated channel walls to avoid nanoparticle accumulation, [5]. An increase in nanoparticle concentration can lead to an increase in thermal conductivity and viscosity and an increase in nanoparticle size, [6]. Nanofluid contribute to the improvement of heat transfer processes, and to reduce and optimize thermal systems. Different properties, such as wettability and thermal conductivity, can be adjusted by altering the nanoparticles concentration, making nanofluids suitable for a wide range of applications, [7]. Nanofluids contains metal or nonmetal particles with nanometer sizes, exhibit much greater thermal conductivity, M. Goodarzi[8]

 doi:10.20944/preprints202107.0517.v1

got an expression for calculating enhanced thermal conductivity of nanofluid has been derived from the general solution of heat conduction equation in spherical coordinates and the equivalent hard sphere fluid model representing the microstructure of particle/liquid mixtures. Researchers have conducted numerous studies to obtain the optimized aspect and states in order to improve heat transfer of equipment and use various nanofluids, [9-15]. The cooling method of microchannel heat sinks combined with nanofluids has become one of the effective ways to solve the heat dissipation problem of high heat flux. Scholars have mainly conducted related research on the influence of the shape of microchannels and the physical properties of nanoparticles on flow and heat transfer characteristics, [16-21]. Shi Xiaojun et al.[22] carried out multi-objective optimization design research on single-layer nanofluid rectangular microchannel. The results show that the pump power and thermal resistance are more sensitive to the channel width and spacing ratio than the aspect ratio. Naphon and Khonseur[23] used air as a cooling medium to conduct an experimental study on the flow and heat transfer characteristics of microchannels with different heights and widths in the Reynolds number range of 200–1,000. The results showed that the height and width of rectangular microchannels exert a significant impact on their heat exchange effect and resistance loss. Studies of this research indicate that, the fluid in the indented sections has a higher heat transfer with the heated wall. Karimipour et al. [24] numerically studied a two-dimensional indented rectangular microchannel. They concluded that by increasing the volume fraction of nanoparticles, the thermal efficiency of nanofluid enhances. Yari Ghale et al. [25]numerically studied the laminar and forced flow of Water/Al_2O_3 nanofluid in an indented microchannel by using two or single phase methods. Their results showed that the Nusselt number and friction factor in an indented microchannel, compared to the smooth microchannel, are higher and these parameters enhance by increasing the width of rib. A segmental analysis pertaining to the heat exchanger takes place to evaluate the influence of nanofluid usage on the heat transfer coefficient, the exchanger's length and its pressure drop. When the volume fraction of Al_2O_3 nanofluids is 5%, the heat transfer coefficient is increased by 10% compared with pure water, and the pressure drop is significantly reduced, [26]. T Raghuraman[27] used pure water as a cooling medium to study the effect of microchannel aspect ratio on heat transfer performance, the study showed that the microchannel aspect ratio influences the heat transfer coefficient, pumping power, pressure drop, and heat transfer performance at different Reynolds numbers. A large aspect ratio can enhance heat transfer, but it can also increase power consumption. Based on the computational fluid dynamics (CFD) method, Mohamadpour J et al. [28] carried out a numerical simulation study on the heat transfer efficiency of the cooperative jet in the microchannel. It was found that increasing the jet frequency and pulse amplitude can significantly improve the heat transfer ability of the microchannel.

In the current work, a rectangular microchannel heat sink is used as the research object, and a three-dimensional flow and heat transfer numerical simulation study is conducted on the basis of the computational fluid dynamics method. Water/Al_2O_3 nanofluid of different concentrations is utilized as the cooling medium, and its influence on the heat transfer performance of microchannels is analyzed. This work also focuses on the evaluation of the flow resistance characteristics and heat transfer laws of microchannels with different aspect ratios. The purpose of the study is to provide theoretical guidance for the optimal design of high heat flux density microchannel heat sinks.

2. Numerical method and model description

2.1. Mathematical model

The single phase fluid model is commonly used to study the flow and heat transfer of nanofluids in microchannels. The nanoparticles in nanofluids are considered to be uniformly distributed in base fluids, and they are in thermal equilibrium. No relative slip

Preprints (www.preprints.org) | NOT PEER-REVIEWED | Posted: 22 July 2021 doi:10.20944/preprints202107.0517.v1

velocity exists between nanoparticles and base liquids, and the flow is regarded as an incompressible steady laminar flow.

Nomenclature	
u_i	velocity components in direction i
u_j	velocity components in direction j
x_i	cartesian coordinate components
x_j	cartesian coordinate components
p	pressure in the flow field
T	temperature
ρ_{nf}	density of nanofluids
μ_{nf}	dynamic viscosity
C_{pf}	specific heat capacity
λ_{nf}	thermal conductivity
w	corresponding thermophysical properties of the base fluid
p	corresponding thermophysical properties of the nanoparticles
α	volume fraction of nanoparticles
n	shape factor of nanoparticles
U_{in}	fluid inlet velocity
q	heat flux
Nu	Nusselt number
N	the number of microchannels
T_s	the temperature of solid region
λ_s	the thermal conductivity of the solid region.

On the basis of these assumptions, the governing equations of nanofluid flow and heat transfer can be expressed as

$$\frac{\partial}{\partial x_j}\left(\rho_{nf} u_j\right) = 0 \tag{1}$$

$$\frac{\partial\left(\rho_{nf} u_i u_j\right)}{\partial x_j} = -\frac{\partial p}{\partial x_i} + \frac{\partial}{\partial x_j}\left[\mu_{nf}\left(\frac{\partial u_i}{\partial x_j} + \frac{\partial u_j}{\partial x_i}\right)\right] \tag{2}$$

$$\frac{\partial}{\partial x_j}\left(\rho_f C_{pf} T u_j\right) = \frac{\partial}{\partial x_j}\left[\lambda_{nf}\frac{\partial T}{\partial x_j}\right] \tag{3}$$

where u_i and u_j are velocity components, x_i and x_j are Cartesian coordinate components, p is the pressure in the flow field, T is the temperature, ρ_{nf} is the density of nanofluids, and μ_{nf} is the dynamic viscosity. C_{pf} is the specific heat capacity, and λ_{nf} is the thermal conductivity. The calculation formula is as follows, [29-30]:

$$\rho_{nf} = (1-\alpha)\rho_w + \alpha\rho_p \tag{4}$$

$$\mu_{nf} = \left(1 + 0.025\alpha + 0.015\alpha^2\right)\mu_w \tag{5}$$

$$C_{pf} = \left[(1-\alpha)(\rho C_p)_w + \alpha\left(\rho C_p\right)_p\right] / \rho_{nf} \tag{6}$$

Preprints (www.preprints.org) | NOT PEER-REVIEWED | Posted: 22 July 2021 doi:10.20944/preprints202107.0517.v1

$$\lambda_{nf} = \frac{\lambda_p + (n-1)\lambda_w - (n-1)\alpha(\lambda_w - \lambda_p)}{\lambda_p + (n-1)\lambda_w + \alpha(\lambda_w - \lambda_p)}\lambda_p \tag{7}$$

The subscripts w and p denote the corresponding thermophysical properties of the base fluid and nanoparticles, respectively. α represents the volume fraction of nanoparticles, and n is the shape factor of nanoparticles. In this work, nanoparticles are regarded as regular spheres with a value of n = 3.

The heat distribution in the solid area of the heat sink can be calculated by the following formula, Ts is the temperature of solid region; λs is the thermal conductivity of the solid region:

$$\frac{\partial}{\partial x_i}\left(\lambda_s \frac{\partial T_s}{\partial x_i}\right) = 0 \tag{8}$$

2.23. D model and boundary conditions

A microchannel heat sink is usually composed of more than 10 or even dozens of microchannels, and its complete modeling and simulation requires a large amount of computing resources. As a result of the symmetry of the model, a typical microchannel heat sink unit can be extracted for simulation. The structure and size of the microchannel heat sink used in this study are shown in Fig. 1. The width W of the heat sink unit is 1 mm, the length L is 50 mm, and the microchannel width W_c is 0.5 mm. The microchannel height W_h values are 5, 10, 15, 20, and 25 mm; they correspond to five different aspect ratios, that is, $HW = W_h/W_c$ with values of 10, 20, 30, 40, and 50 respectively. The bottom height of the heat sink is set at 6 mm. Symmetrical boundary conditions are set on both sides of the heat sink, and a uniform heat flux q = 0.8 MW/m² is set at the bottom. The top wall is set as the adiabatic boundary. The inlet of the microchannel fluid adopts velocity inlet boundary, the inlet fluid temperature is set at 300 K, the outlet of the microchannel fluid is set as pressure outlet, the upper wall of the fluid domain adopts adiabatic solid wall boundary condition, and the interface between fluid and solid adopts coupled heat flow coupling boundary condition. In this paper, ICEM CFD software is used for 3D modeling and mesh generation, and the general CFD software FLUENT 15.0 is used for numerical simulation. According to the geometric models with different aspect ratios, three sets of grids are divided to analyze the grid independence under the maximum Reynolds number.

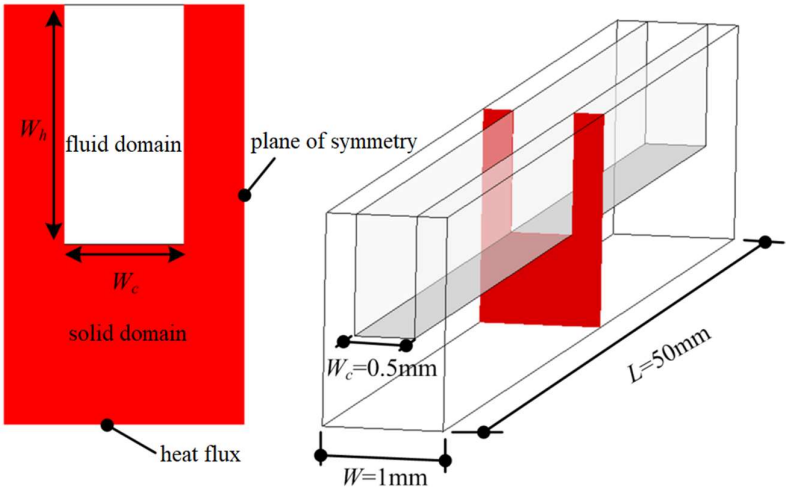

Figure 1. Schematic of heat sink with square cross section.

2.2. Model validation

 doi:10.20944/preprints202107.0517.v1

The experimental data of Lei [31] are used for comparison to verify the prediction performance of the mathematical model. The microchannel width W_c is 0.1 mm, the height W_h is 0.5 mm, the length L is 10 mm, and the heat flux q at the bottom of the heat sink is 0.6 MW/m^2. The cooling medium is pure water. In the calculation, the volume fraction of the nanoparticles α is 0.

The characteristic scale of microchannels can be defined as

$$D_h = \frac{2W_h W_c}{W_h + W_c} \tag{9}$$

The microchannel Reynolds number is

$$Re = \frac{\rho_f U_{in} D_h}{\mu_f} \tag{10}$$

where U_{in} is the fluid inlet velocity.

The average temperature T_c of the liquid–solid heat transfer surface and the average temperature T_f of the whole microchannel fluid can be respectively defined as

$$T_c = \frac{\int T dA}{\int dA} \tag{11}$$

$$T_f = \frac{\int \rho_f T dV}{\int \rho_f dV} \tag{12}$$

Therefore, the average heat transfer coefficient can be expressed as

$$h = \frac{qA_b}{A_c (T_c - T_f)} \tag{13}$$

where A_b is the heating area of the bottom of the thermal sink and A_c is the heat exchange area between the fluid domain and the solid domain in the microchannel.

The average Nusselt number is defined as follows:

$$Nu = \frac{hD_h}{\lambda_f} \tag{14}$$

The comparison between the average Nusselt number predicted by the mathematical model and the experimental results is shown in Fig. 2. The results show that the proposed model achieves certain accuracy and reliability in the prediction of fluid laminar flow and heat transfer in microchannels.

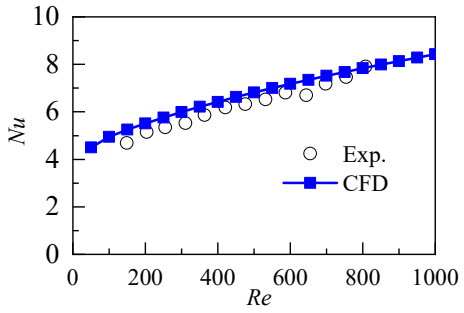

Figure 2. Model validation by comparing the present results with Lei et al. experiments[31].

 doi:10.20944/preprints202107.0517.v1

3. Result analysis and discussion

3.1. Influence of nanoparticle volume fraction

Take the microchannel heat sink with aspect ratio HW = 10（$HW = W_h/W_c$）as an example. The three-dimensional flow and heat transfer of the nanofluids are simulated in the Reynolds number range of 100–500, and the nanoparticle volume fractions α are 0.5% and 5%, respectively. According to formula 10, Reynolds number is directly related to density, inlet velocity, characteristic scale and viscosity, while density and viscosity are related to the content of solid particles in nanofluids. In this paper, the physical properties of the fluid and the characteristic scale of the channel are determined by giving the solid particle content and aspect ratio in the nanofluid. Finally, the Reynolds number can be changed by adjusting the inlet velocity. The temperature distributions in the middle section of the heat sink are extracted for comparison, and the results are shown in Fig. 3. The laws of the temperature distributions in the middle sections of two types of nanofluids at different Reynolds numbers are similar. The temperature at the bottom of the heat sink is the highest, and the temperature in the solid region decreases gradually along the height of the microchannel. The temperature of the fluid at the center of the fluid domain of the microchannel is relatively low. At the fluid structure coupling heat transfer surface, the fluid temperature is relatively high because of the heating of the solid surface. At the same time, with the increase of the Reynolds number, the heat sink temperature and fluid temperature decrease significantly. When the Reynolds number remains the same, the heat sink temperature and fluid temperature of the nanofluid with a nanoparticle volume fraction of 5% are significantly lower than those of the nanofluid with a nanoparticle volume fraction of 0.5%.

The average temperature on the heat exchange surface of the fluid and solid domains under each working condition is obtained. The results are shown in Fig. 4. With the increase of the Reynolds number, the average temperature on the heat transfer surface of the two types of nanofluids decreases. At the same Reynolds number, increasing the volume fraction of nanoparticles in the nanofluid can reduce the temperature on the heat transfer surface. In the range of Reynolds number studied in this work, the average temperature difference on the heat transfer surface caused by the differences in nanoparticle volume fraction decreases with the increase of the Reynolds number. When Re is 100, the average temperature difference between the nanofluid with a nanoparticle volume fraction of 5% and that with a nanoparticle volume fraction of 0.5% is 6.3 K. When Re is 500, the average temperature difference of the heat exchange surface decreases to 2.6 K. This result shows that the average temperature of the heat exchange surface can be reduced by increasing the nanoparticle volume fraction under the condition with a low Reynolds number.

Fig. 5 shows the effects of nanoparticle volume fraction on heat transfer coefficients with different Reynolds numbers. The results show that the average heat transfer coefficient increases with the increase of the Reynolds number and that the increase of the nanoparticle volume fraction can improve the heat transfer ability of the nanofluids. As shown in Figure 6, in order to comprehensively consider the difference of fluid thermal conductivity caused by different volume fraction of nanoparticles, Nusselt number is used as the evaluation index for comparative analysis, and the same conclusion can be obtained.

Fig. 7 shows the distribution of the pressure difference between the inlet and outlet of the microchannel with different volume fractions. The drag loss of nanofluids through microchannels increases with the increase of Reynolds number. However, the drag loss of nanofluids with a nanoparticle volume fraction of 5% is greater than that of nanofluids with a nanoparticle volume fraction of 0.5%. At the same time, because the volume fraction of nanoparticles affects the density and dynamic viscosity of nanofluids, the velocity of the microchannel inlet must be adjusted to keep the same Reynolds number. As shown in Fig. 8, with the increase of the Reynolds number, the inlet velocity of the 5% nanofluid

Preprints (www.preprints.org) | NOT PEER-REVIEWED | Posted: 22 July 2021 doi:10.20944/preprints202107.0517.v1

is greater than that of the 0.5% nanofluid. Pumping power is introduced as the evaluation index to reasonably evaluate the synergistic effect of inlet velocity and resistance loss. Its physical meaning is the external work required for nanofluids to pass through microchannels. Pumping power p is expressed as:

$$P = N \cdot U_{\text{in}} \cdot W_{\text{h}} \cdot W_{\text{c}} \cdot_{\Delta} p \tag{15}$$

N is the number of microchannels in the whole heat sink, and the value is N = 1.

The variation of pumping power with the Reynolds number is shown in Fig. 9. With the increase of the Reynolds number, the pumping power of the nanofluid with a nanoparticle volume fraction of 5% is significantly higher than that of the nanofluid with a nanoparticle volume fraction of 0.5%. This result shows that the heat transfer performance cannot be improved by increasing the nanoparticle volume fraction because doing so greatly increases the power consumption of the whole system. At the same time, a high volume fraction renders the nanoparticles in nanofluids unable to maintain a stable and uniform suspension state, [31]. Therefore, in engineering applications, the nanoparticle volume fraction in nanofluids needs to be maintained at a low level.

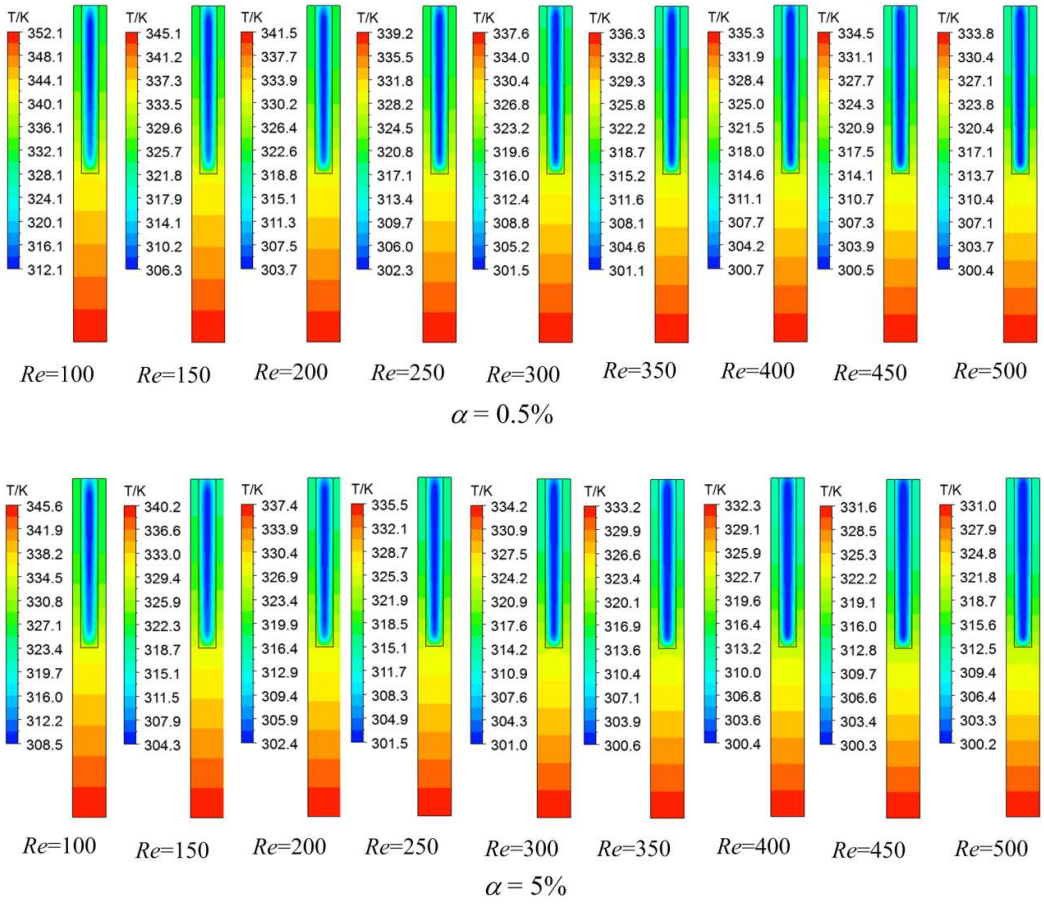

Figure 3. Temperature distributions of fluid and solid domains at the middle plane.

Preprints (www.preprints.org) | NOT PEER-REVIEWED | Posted: 22 July 2021 doi:10.20944/preprints202107.0517.v1

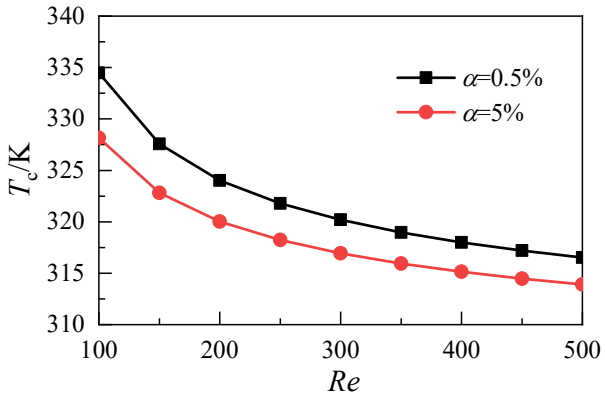

Figure 4. Average temperature distributions of fluid–solid surface.

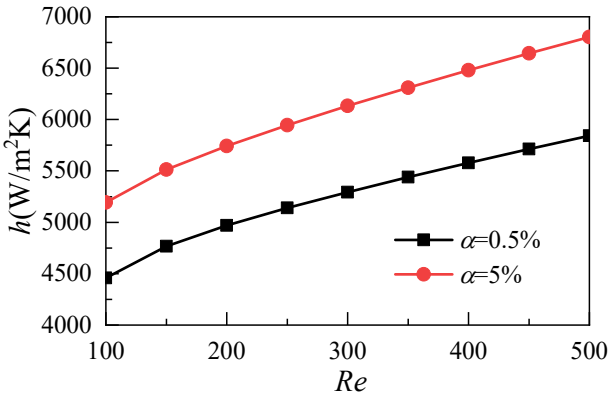

Figure 5. Effects of nanoparticle volume fraction on heat transfer coefficients.

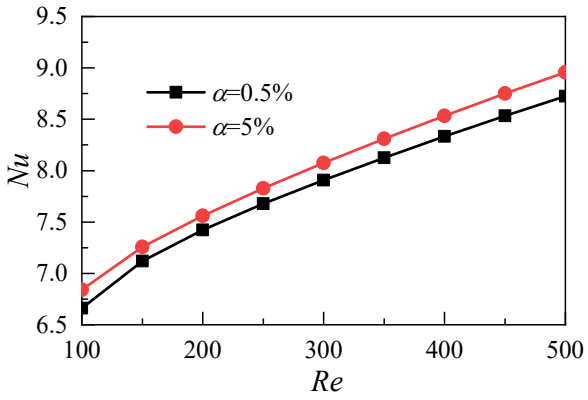

Figure 6. Influence of nanoparticle volume fraction on Nusselt number.

Preprints (www.preprints.org) | NOT PEER-REVIEWED | Posted: 22 July 2021 doi:10.20944/preprints202107.0517.v1

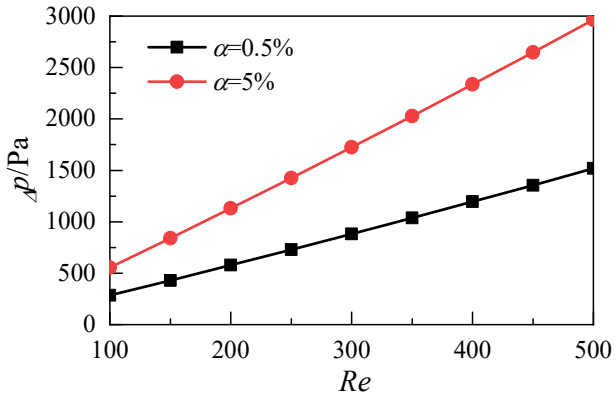

Figure 7. Influence of nanoparticle volume fraction on pressure difference.

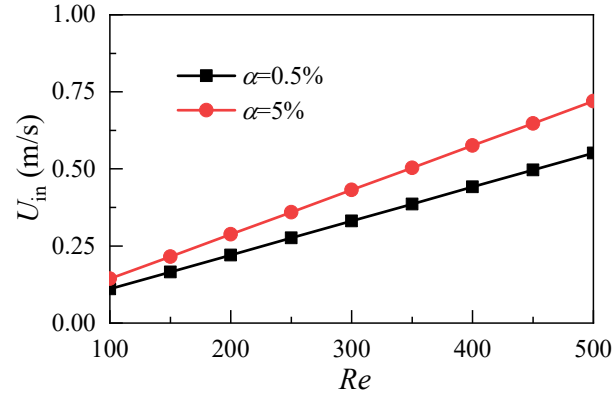

Figure 8. Effect of nanoparticle volume fraction on inlet velocity.

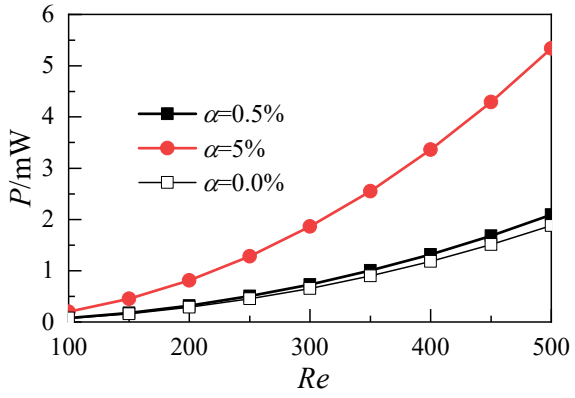

Figure 9. Effects of nanoparticle volume fraction on pumping power.

3.2. Influence of the aspect ratio of microchannels

This work studies nanofluids with a nanoparticle volume fraction of 5%. The different aspect ratios *HW* of microchannels can be obtained by changing their height W_h. The aspect ratios *HW* of the five microchannel heat sink models are 10, 20, 30, 40, and 50. A three-dimensional simulation of flow and heat transfer under different Reynolds numbers

 doi:10.20944/preprints202107.0517.v1

is conducted, and the flow and heat transfer characteristics of nanofluid microchannels with aspect ratio are analyzed and compared. As shown in Fig. 10, the pressure difference between the inlet and the outlet increases with the increase of the Reynolds number under different aspect ratios of the microchannel heat sink. The pressure difference decreases with the increase of the aspect ratio at the same Reynolds number. When the aspect ratio is 20–50, the pressure difference is not obvious. This result shows that the increase of the aspect ratio of the microchannel does not greatly enhance the flow resistance loss of nanofluids under the parameters studied in this work. Fig. 11 shows the variation of the resistance coefficient f of the microchannel with the Reynolds number. The simulation results of the five different aspect ratios show that the drag coefficient decreases with the increase of the Reynolds number. Moreover, the differences in the drag coefficients caused by different aspect ratios decrease with the increase of the Reynolds number.

Fig. 12 shows the variation of the average temperature at the bottom of the microchannel heat sink with the Reynolds number at different aspect ratios. The results show that the bottom mean temperature corresponding to the five microchannel heat sinks decreases with the increase of the Reynolds number and that increasing the aspect ratio of the microchannel can reduce the bottom temperature of the heat sink. However, when the aspect ratio exceeds 20, the decrease of the heat sink's bottom temperature caused by an increase in the aspect ratio of the microchannel obviously drops, and the average temperature values of the bottom of the three microchannel heat sinks with aspect ratios of 30, 40, and 50 almost coincide.

The average temperature distribution of the fluid–solid surface relative to the heat transfer in the microchannels with different aspect ratios is shown in Fig. 13. With the increase of the Reynolds number, the average temperature of the heat transfer surface decreases. When the aspect ratio *HW* increases from 10 to 20, the corresponding temperature drop is 16.8 K at Re of 100. When the aspect ratio *HW* increases from 20 to 30, the corresponding temperature drop is 5.7 K. When the aspect ratio *HW* increases from 30 to 40, the corresponding temperature drop decreases to 2.9 K. When the aspect ratio *HW* increases from 40 to 50, the corresponding temperature drop further decreases to 1.8 K. As shown in Fig. 14, when the aspect ratio *HW* increases from 10 to 30, the Nusselt number increases. When the aspect ratio further increases from 30 to 50, the Nusselt number does not increase significantly. This result indicates that the increase of the aspect ratio does not significantly improve the heat transfer performance of the microchannel heat sink in this range. The above analysis shows that the change of the aspect ratio of the microchannel affects its heat transfer performance and resistance characteristics. In this work, the comprehensive heat transfer performance index is used to quantitatively evaluate the synergistic effect. It is defined as

$$\eta = \frac{\left(Nu / Nu_0\right)}{\left(f / f_0\right)^{1/3}} \tag{16}$$

where f_0 is the resistance coefficient of the microchannel with aspect ratio $HW = 10$ and Nu_0 is the average Nusselt number of the microchannel with aspect ratio $HW = 10$.

Fig. 15 shows the variations of the comprehensive heat transfer performance parameters of the microchannel heat sinks with different aspect ratios and given different Reynolds numbers. In the range of the Reynolds number studied in this work, the comprehensive heat transfer performance parameters are greater than 1. The results indicate that for the microchannel heat sink with $HW = 10$, increasing the aspect ratio can improve its comprehensive heat transfer performance. When the aspect ratio is increased to 30, the comprehensive heat transfer performance of the microchannel heat sink does not continue to improve.

Preprints (www.preprints.org) | NOT PEER-REVIEWED | Posted: 22 July 2021 doi:10.20944/preprints202107.0517.v1

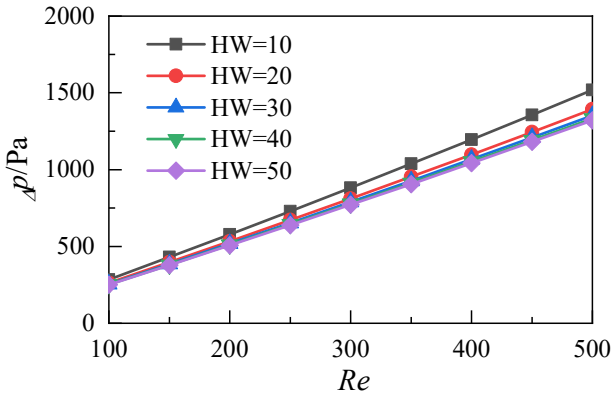

Figure 10. Distributions of pressure difference between the inlet and the outlet of the microchannel heat sink with different aspect ratios.

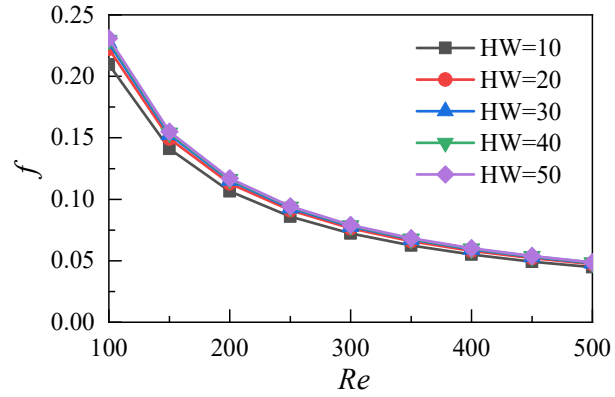

Figure 11. Distributions of friction coefficients.

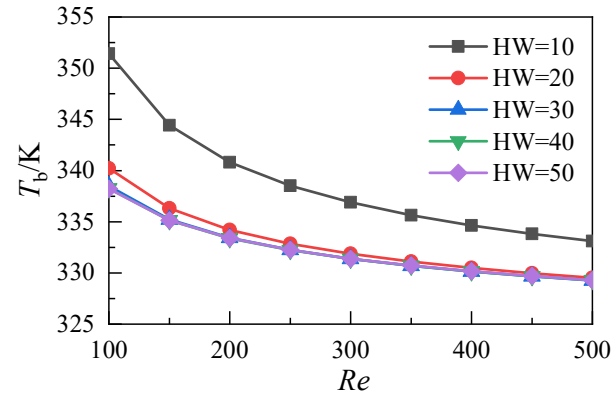

Figure 12. Temperature distributions of the heat sink bottom with different aspect ratios.

Preprints (www.preprints.org) | NOT PEER-REVIEWED | Posted: 22 July 2021 doi:10.20944/preprints202107.0517.v1

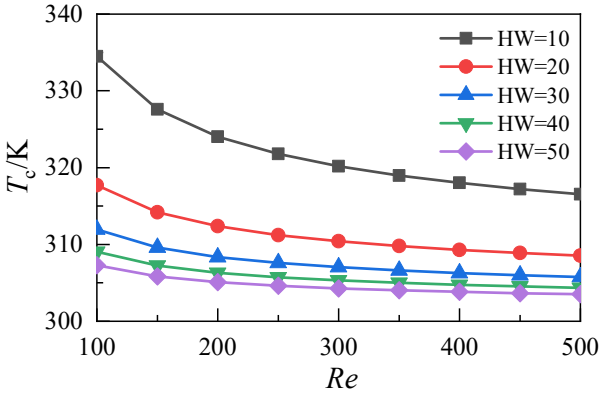

Figure 13. Temperature distributions of fluid–solid surface in microchannels with different aspect ratios.

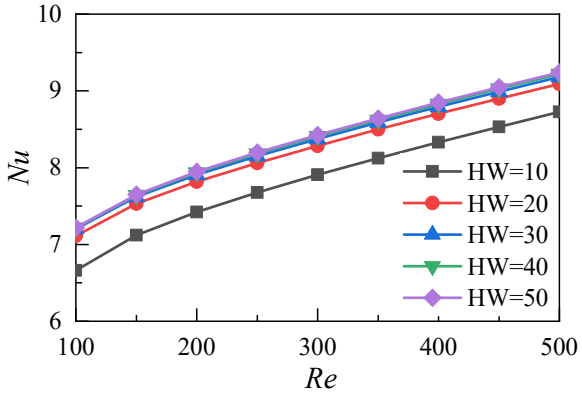

Figure 14. Nusselt number distributions of microchannels with different aspect ratios.

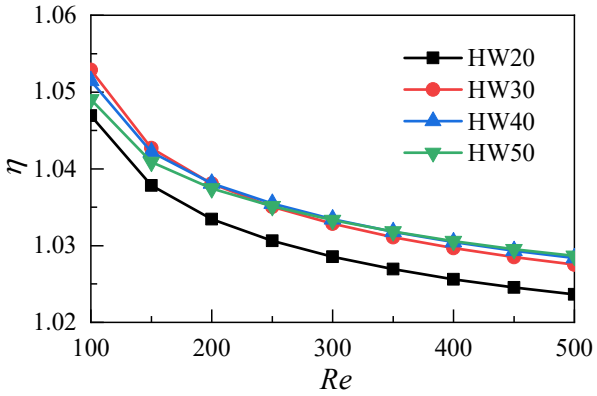

Figure 15. Comparisons of comprehensive heat transfer performances of microchannels with different aspect ratios.

4. Conclusion

In this work, a microchannel heat sink is studied on the basis of computational fluid dynamics. The flow and heat transfer of two nanofluids with different volume fractions and five microchannel heat sinks with different aspect ratios in the Reynolds number range of 100–500 are simulated. The flow and heat transfer characteristics of the

microchannel heat sinks are compared, and the optimal parameters of the aspect ratio are analyzed. The conclusions are as follows:

(1) Increasing the volume fraction of nanoparticles can effectively reduce the average temperature of the heat transfer surface and improve the heat transfer capability of nanofluids. However, because of the dual increase of the inlet velocity and flow resistance, the power consumption of the whole system increases greatly;

(2) Increasing the aspect ratio of the microchannel does not cause significant flow resistance loss, and the resistance coefficient of the microchannel tends to be consistent with the increase of the Reynolds number at different aspect ratios;

(3) Increasing the aspect ratio of the microchannel can reduce the temperature of the heat sink. When the aspect ratio exceeds 30, the average temperature at the bottom of the microchannel does not decrease, and the heat transfer coefficient does not increase;

(4) In the range of the parameters studied in this paper, the aspect ratio of the microchannel heat sink with a thickness of 6 mm has an optimal value. Based on the comprehensive heat transfer performance parameters, the optimal value of the aspect ratio of the microchannel heat sink is 30.

This study shows that the aspect ratio of heat sink has a significant impact on the heat transfer performance of microchannel, and there is an optimal value in the range of Reynolds number under the condition of given thickness. Further research will be carried out for different thickness of heat sink under different Reynolds number conditions to obtain a universal empirical formula for guiding engineering practice.

Acknowledgments: The authors acknowledge the support of the 14th batch High-level Talents Project for "Six Talents Peak" (Grant No. XCL-092), the Province Postdoctoral Foundation of Jiangsu (1501164B), the Technical Innovation Nurturing Foundation of Yangzhou University (2017CXJ024), China Postdoctoral Science Foundation (2016M600447), Yangzhou Innovative Capacity Building Plan Project (YZ2017275) and Yangzhou University Science Foundation Project (x20180290).

References

[1]. Wu R , Hong T , Cheng Q , et al. Thermal modeling and comparative analysis of jet impingement liquid cooling for high power electronics[J]. International Journal of Heat & Mass Transfer, 2019, 137(JUL.):42-51.

[2]. Choi T J , Kim S H , Jang S P , et al. Heat Transfer Enhancement of a Radiator with Mass-Producing Nanofluids (EG/water-based Al2O3 Nanofluids) for Cooling a 100 kW High Power System[J]. Applied Thermal Engineering, 2020, 180:115780.

[3]. Tuckerman D B , Pease R . High-performance heat sinking for VLSI[J]. IEEE Electron Device Letters, 1981, 2(5):126-129.

[4]. Choi S , Eastman J A . Enhancing thermal conductivity of fluids with nanoparticles[J]. ASME International Mechanical Engineering Congress & Exposition, 1995.

[5]. J. Koo,C. Kleinstreuer. Laminar nanofluid flow in microheat-sinks[J]. International Journal of Heat and Mass Transfer,2005,48(13):2652–2661.

[6]. Apmann Kevin, Fulmer Ryan, Soto Alberto, Vafaei Saeid. Thermal Conductivity and Viscosity: Review and Optimization of Effects of Nanoparticles.[J]. Materials (Basel, Switzerland),2021,14(5):1291-1362.

[7]. A. Malvandi, M.R. Safaei, M.H. Kaffash, D.D. Ganji, MHD mixed convection in a vertical annulus filled with Al2O3-water nanofluid considering nanoparticle migration, J. Magn. Magn. Mater. 382 (2015) 296–306.

[8]. M. Goodarzi, A. Amiri, M.Sh. Goodarzi, M.R. Safaei, A. Karimipour, E. MohseniLanguri, M. Dahari, Investigation of heat transfer and pressure drop of a contour flow corrugated plate heat exchanger using MWCNT based nanofluids, Int. Commun. Heat Mass Transfer 66 (2015) 172–179.

[9]. M.H. Esfe, A. Karimipour,W.M. Yan, M. Akbari, M.R. Safaei, M. Dahari, Experimental study on thermal conductivity of ethylene glycol based nanofluids containing Al2O3 nanoparticles, Int. Commun. Heat Mass Transfer 88 (2015) 728–734.

[10]. M.H. Esfe, S. Wongwises, A. Naderi, A. Asadi, M.R. Safaei, H. Rostamian, M. Dahari, A. Karimipour, Thermal conductivity of Cu/TiO2-water-EG hybrid nanofluid: experimental data and modeling using artificial neural network and correlation, Int. Commun. Heat Mass Transfer 66 (2015) 100–104.

[11]. M.R. Safaei, O. Mahian, F. Garoosi, K. Hooman, A. Karimipour, S.N. Kazi, S. Gharehkhani, Investigation of micro and nano-

sized particle erosion in a 90° pipe bend using a two phase discrete phase model, Sci. World J. 2014 (2014) 11, 740578.
[12]. M.R. Safaei, Hussein Togun, K. Vafai, S.N. Kazi, A. Badarudin, Investigation of heat transfer enchantment in a forward-facing contracting channel using FMWCNT nanofluids, Numer. Heat Transfer, Part A 66 (2014) 1321–1340.
[13]. A. Raisia, S.M. Aminossadati, B. Ghasemi, An innovative nanofluid-based cooling using separated natural and forced convection in low Reynolds flows, J. Taiwan Inst. Chem. Eng. (2016) http://dx.doi.org/10.1016/j.jtice.2016.02.014.
[14]. S.A. Sajadifar, A. Karimipour, D. Toghraie, Fluid flow and heat transfer of non-Newtonian nanofluid in a microtube considering slip velocity and temperature jump boundary conditions, Eur. J. Mech. B. Fluids 61 (2017) 25–32.
[15]. S. Oveissi, D. Toghraie, S.A. Eftekhari, Longitudinal vibration and stability analysis of carbon nanotubes conveying viscous fluid, Physica E: Low-dimensional Systems and Nanostructures 83 (2016) 275–283.
[16]. Gravndyan, Qumars, Akbari, et al. The effect of aspect ratios of rib on the heat transfer and laminar water/TiO_2 nanofluid flow in a two-dimensional rectangular microchannel[J]. Journal of Molecular Liquids, 2017.
[17]. A. Aghanajafi, D. Toghraie, B. Mehmandoust, Numerical simulation of laminar forced convection of water-CuO nanofluid inside a triangular duct, Physica E: Low-dimensional Systems and Nanostructures 85 (2017) 103–108.
[18]. Heydari A , Akbari O A , Safaei M R , et al. The effect of attack angle of triangular ribs on heat transfer of nanofluids in a microchannel[J]. Journal of Thermal Analysis & Calorimetry, 2017.
[19]. Naphon P , Khonseur O . Study on the convective heat transfer and pressure drop in the micro-channel heat sink[J]. International Communications in Heat & Mass Transfer, 2009, 36(1):39-44.
[20]. Raghuraman D , Thundil K , Nagarajan P K , et al. Influence of aspect ratio on the thermal performance of rectangular shaped micro channel heat sink using CFD code[J]. Alexandria Engineering Journal, 2016:S1110016816302447.
[21]. A. Karimipour, H. Alipour, O.A. Akbari, D. Toghraie Semiromi, M.H. Esfe, Studying the effect of indentation on flow parameters and slow heat transfer of Water-silver nanofluid with varying volume fraction in a rectangular two-dimensional microchannel, Ind. J. Sci. Tech. 8 (15) (2015) 51707 July.
[22]. Shi Xiaojun, Li Shan, Wei Yadong, et al. Multi objective optimization of structural parameters of nanofluid rectangular microchannel heat sink [J]. Journal of Xi'an Jiaotong University, 2018, 52 (05): 61-66.
[23]. Z. YariGhale, M. Haghshenasfard, M. Nasr Esfahany, Investigation of nanofluids heat transfer in a ribbed microchannel heat sink using singlephase and multiphase CFD models, Int. Commun. Heat Mass Transfer 68 (2015) 122–129.
[24]. O. Manca, S. Nardini, D. Ricci, A numerical study of nanofluid forced convection in ribbed channels, Appl. Therm. Eng. 37 (2012) 280–292.
[25]. Huaqing Xie,Motoo Fujii,Xing Zhang. Effect of interfacial nanolayer on the effective thermal conductivity of nanoparticle-fluid mixture[J]. International Journal of Heat and Mass Transfer,2004,48(14):2926–2932.
[26]. Gkountas Apostolos A, Th. Benos Lefteris, Nikas Konstantinos Stefanos, Sarris Ioannis E.. Heat transfer improvement by an Al2O3-water nanofluid coolant in printed-circuit heat exchangers of supercritical CO2 Brayton cycle[J]. Thermal Science and Engineering Progress,2020,20(5):1025-1051.
[27]. Sohel M R , Khaleduzzaman S S , Saidur R , et al. An experimental investigation of heat transfer enhancement of a minichannel heat sink using Al_2O_3–H_2O nanofluid[J]. International Journal of Heat and Mass Transfer, 2014, 74(JUL):164-172.
[28]. Mohammadpour J , Salehi F , Sheikholeslami M , et al. Optimization of nanofluid heat transfer in a microchannel heat sink with multiple synthetic jets based on CFD-DPM and MLA[J]. International Journal of Thermal Sciences, 2021, 167(1):107008.
[29]. Khanafer K , Vafai K . A critical syn study of thermophysical characteristics of nanofluids[J]. International Journal of Heat and Mass Transfer, 2011, 54(19-20):4410-4428.
[30]. Lei C , Xia G , Liang W , et al. Heat transfer enhancement in microchannel heat sinks with periodic expansion-constriction cross-sections[J]. International Journal of Heat & Mass Transfer, 2013, 62(JUL.):741-751.
[31]. Lee J , Mudawar I . Assessment of the effectiveness of nanofluids for single-phase and two-phase heat transfer in micro-channels[J]. International Journal of Heat & Mass Transfer, 2007, 50(3/4):452-463.